Supporting information for

Silicon Phthalocyanine-based *N*-Type Organic Mixed Ionic-Electronic Conductor in Organic Electrochemical Transistors

May Ourabi[a], Mario C. Vebber[a,b], Mélanie Cyr[a,b], Forest St-Denis Weintrager[a], Nicolas Ledos[a,b], Halynne R. Lamontagne[a,b], Audithya Nyayachavadi[a], Jaclyn L. Brusso[b] and Benoît H. Lessard[a,c]*

[a] Department of Chemical and Biological Engineering, University of Ottawa, 161 Louis Pasteur, Ottawa, ON, Canada.

[b] Department of Chemistry and Biomolecular Sciences, University of Ottawa 150 Louis Pasteur, Ottawa, ON, Canada.

[c] School of Electrical Engineering and Computer Science, University of Ottawa, 800 King Edward Ave., Ottawa, ON, Canada.

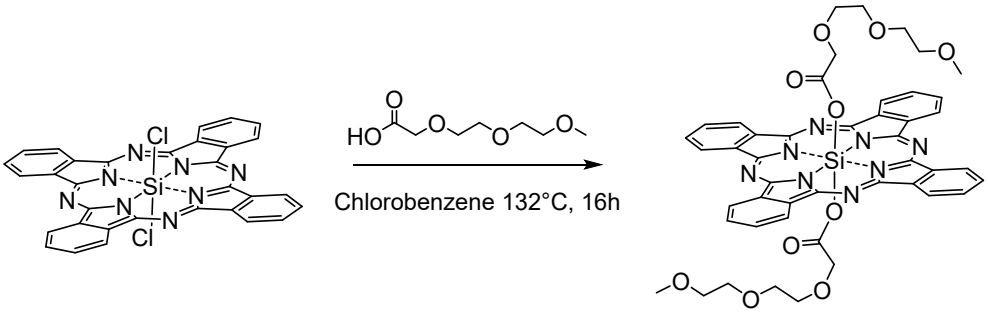

Figure S1. *Synthetic scheme of MEEA-SiPc from Cl_2-SiPc.*

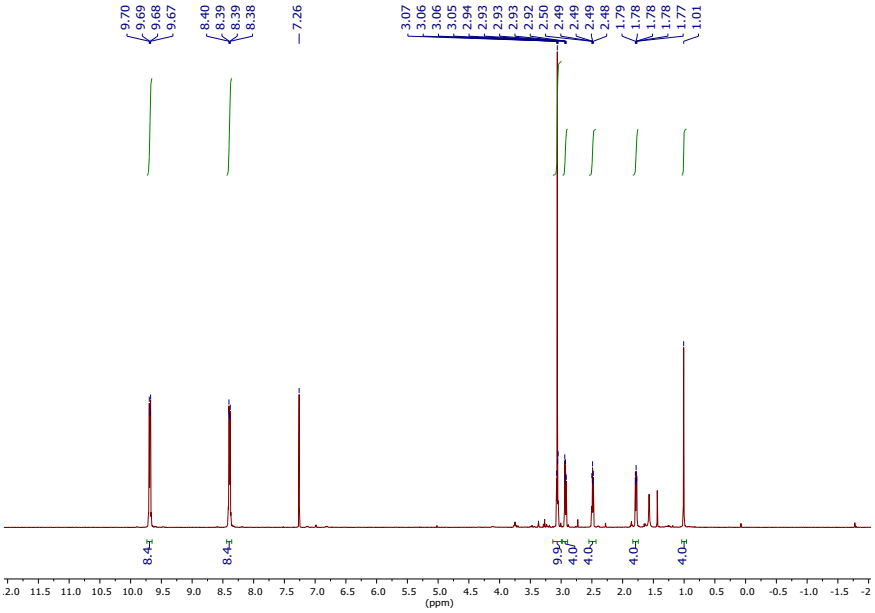

Figure S2. *^{1}H-NMR spectrum of MEEA-SiPc in deuterated chloroform.*

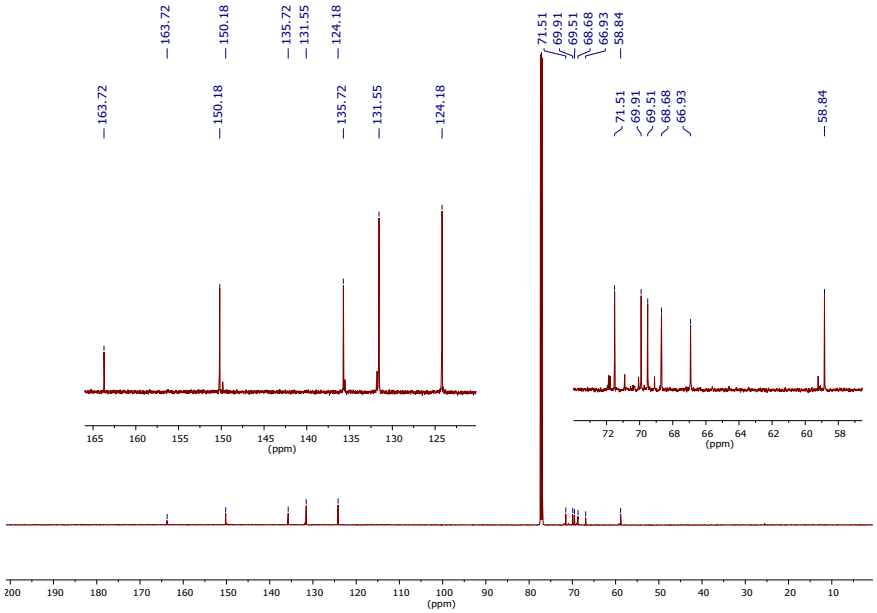

Figure S3. *^{13}C-NMR spectrum of MEEA-SiPc in deuterated chloroform.*

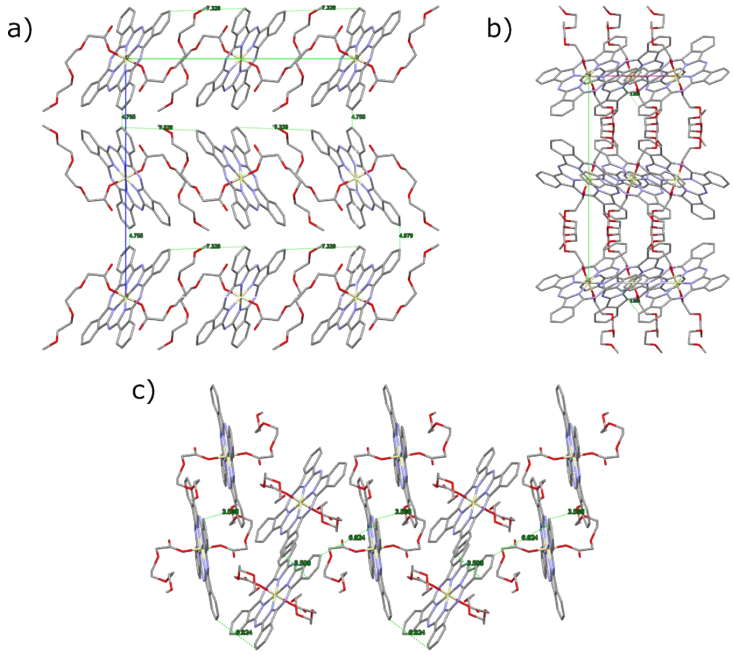

Figure S4. *View along a) a-axis and b) c-axis of the MEEA-SiPc crystal structure obtained from single crystal XRD. c) Reproduction of the view in Figure 2e with measured distances. Hydrogen atoms have been hidden in this representation.*

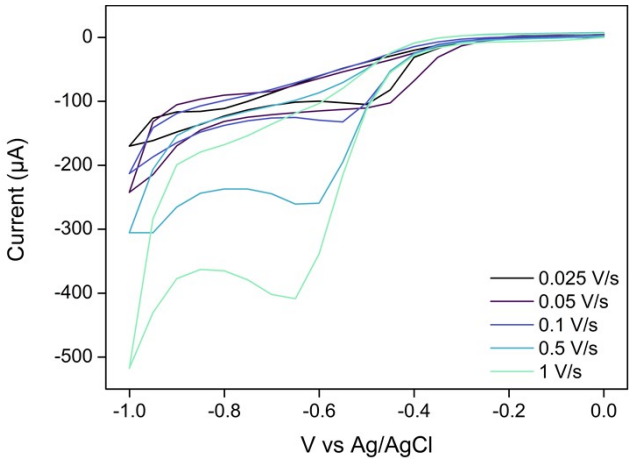

Figure S5. *Cyclic voltammetry of an MEEA-SiPc film cast on ITO-glass in 0.1 M NaCl solution.*

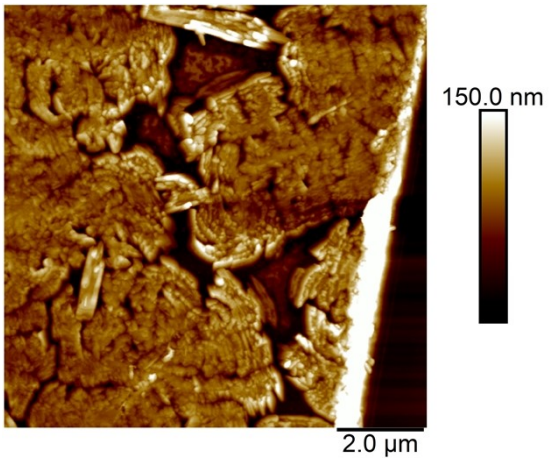

Figure S6. *10 × 10 μm AFM imaging of the pristine MEEA-SiPc film adjacent to an exposed area of the substrate (right side).*

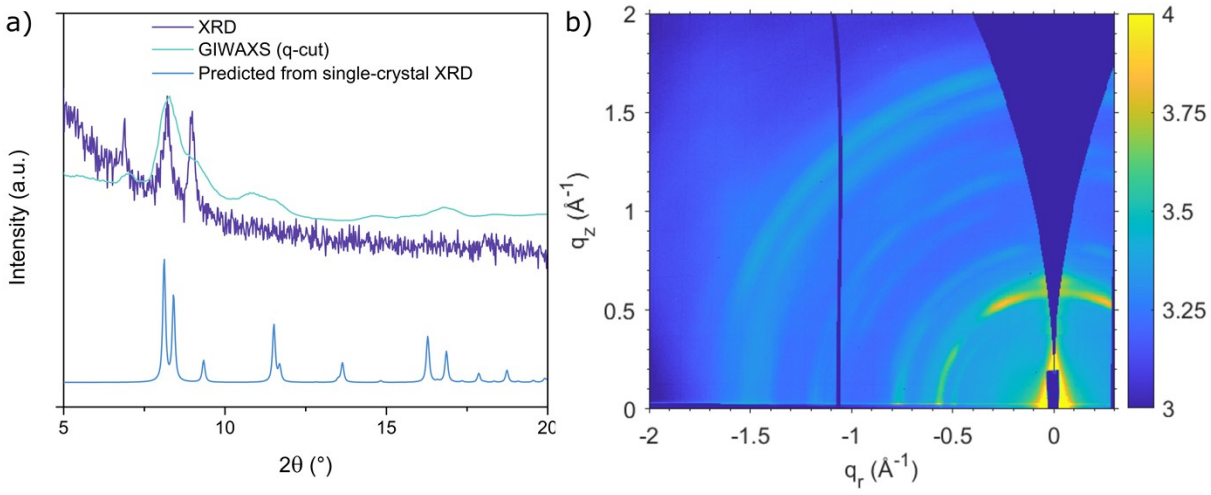

Figure S7. *a) Diffraction pattern of MEEA-SiPc obtained from XRD and GIWAXS on an Si substrate. Both spectra are compared to the predicted diffraction pattern obtained from single crystal XRD. Data collected from GIWAXS was corrected to account for different excitation wavelengths, from λ=1.24 Å^{-1},to λ=1.54 Å^{-1}. b) 2D GIWAXS scattering pattern of MEEA-SiPc on an Si substrate.*

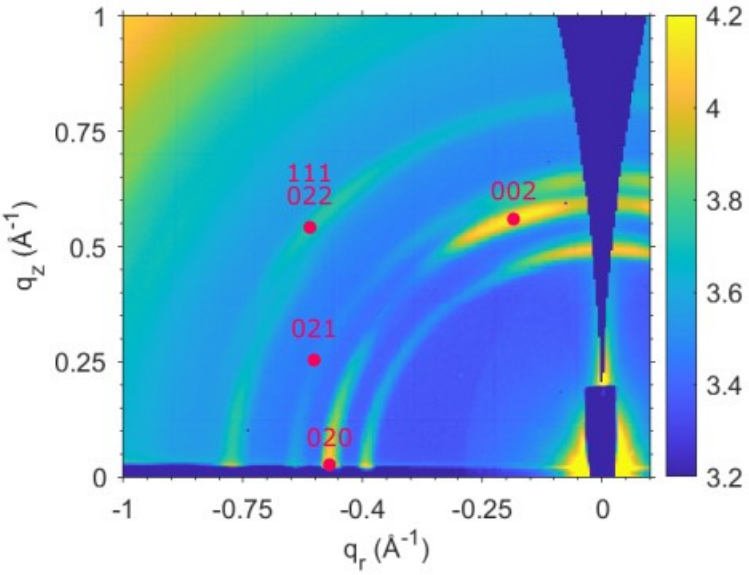

Figure S8. *Peak assignment identified from single-crystal data.*

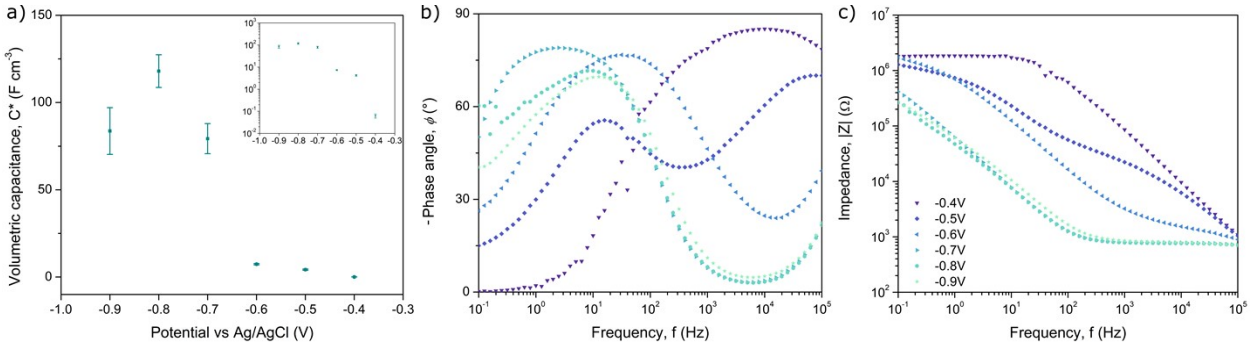

Figure S9. *a) Change in extracted volumetric capacitance (C*), b) phase angle and c) impedance as a function of applied voltage. Data from -0.1 V to -0.3 V were discarded due to high levels of noise in the measurements.*

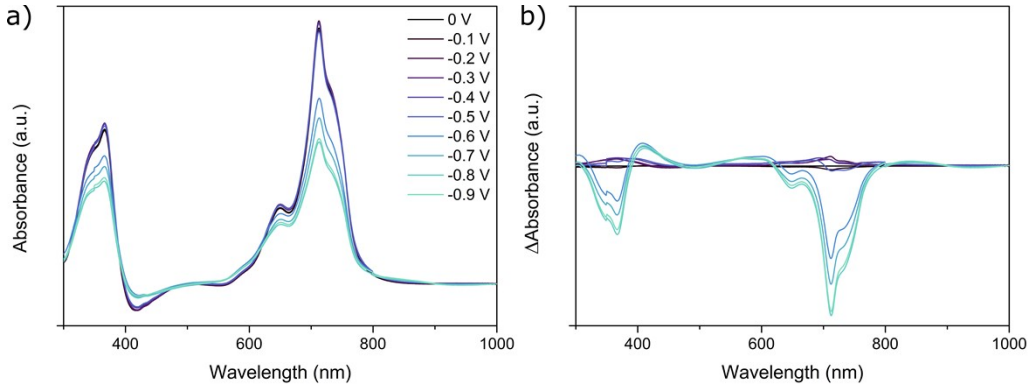

Figure S10. *Spectroelectrochemistry results obtained from the MEEA-SiPc film on ITO-glass. a) Absorbance and b) difference in absorbance vs. data at* $V_{applied}$ *= 0 V as a function of applied voltage.*

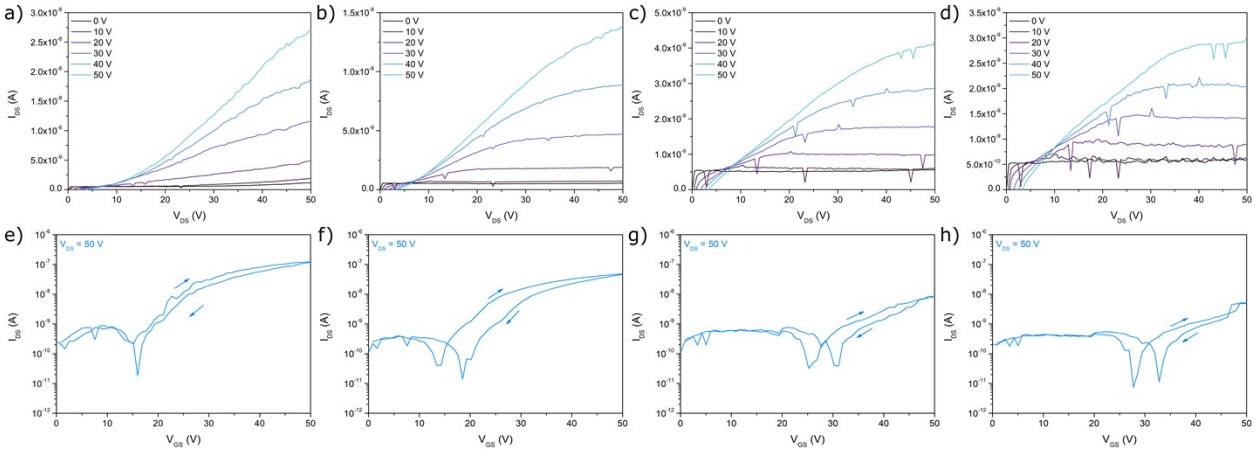

Figure S11. *Output and transfer curves obtained from MEEA-SiPc OTFT devices with channel lengths of a,e) 2.5 µm, b,f) 5 µm, c,g) 10 µm and d,h) 20 µm.*

Table S1. *OTFT device performance.*

Channel length* **[µm]**	$\mu_e \times 10^{-5}$ **[cm^2 V^{-1} s^{-1}]**	V_T **[V]**	$I_{on/off}$ **[-]**
2.5	1.01 ± 0.14	6.6 ± 1.7	10^2
5	0.67 ± 0.06	6.5 ± 1.8	10^2
10	0.98 ± 0.09	22.4 ± 2.8	10^1
20	0.43 ± 0.15	23.2 ± 1.7	10^0-10^1

**n* = 4 devices for each channel length.

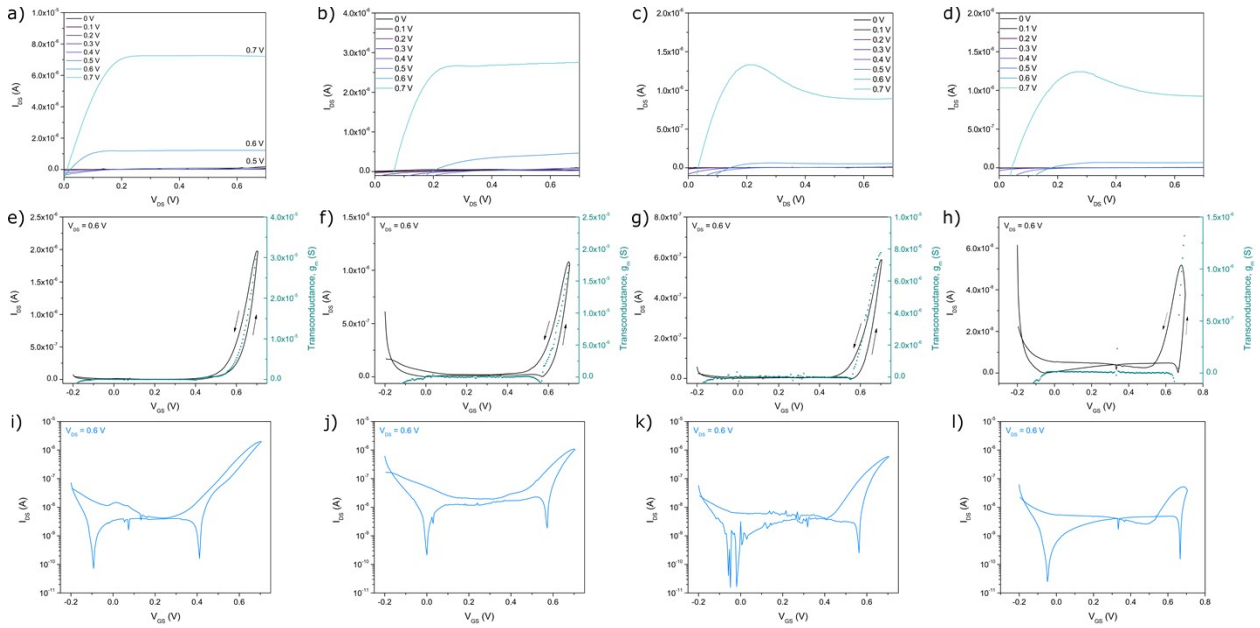

Figure S12. *Output curves obtained from MEEA-SiPc OECT devices with channel lengths of a) 2.5 µm, b) 5 µm, c) 10 µm and d) 20 µm. Transfer curves plotted on linear and logarithmic scales obtained from MEEA-SiPc OECT devices with channel lengths of e,i) 2.5 µm, f,j) 5 µm, g,k) 10 µm and h,l) 20 µm.*

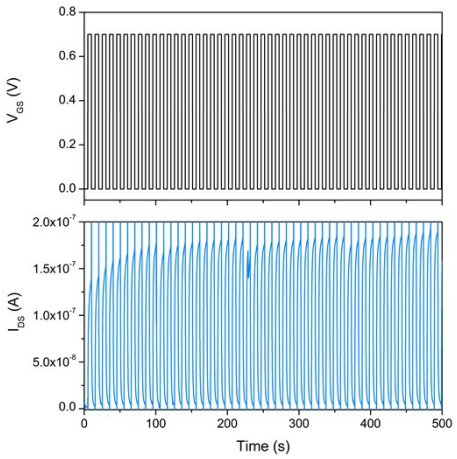

Figure S13. *Transient characteristics of the 5wt%PEG/MEEA-SiPc OECT with W = 10 mm, L = 2.5 µm.*

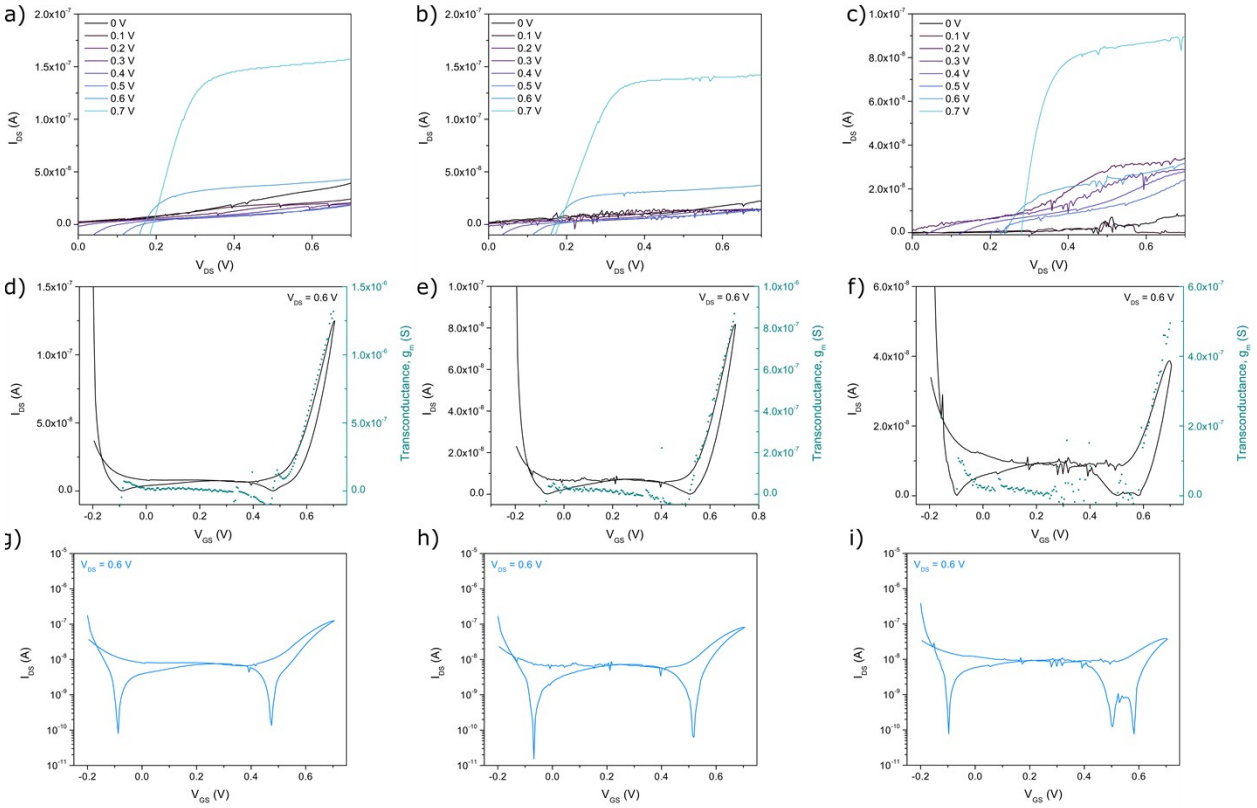

Figure S14. *Output curves obtained from 5wt%PEG/MEEA-SiPc OECT devices with channel lengths of a) 2.5 µm, b) 5 µm and c) 10 µm. Transfer curves plotted on linear and logarithmic scales obtained from 5wt%PEG/MEEA-SiPc OECT devices with channel lengths of d,g) 2.5 µm, e,h) 5 µm and f,i) 10 µm.*